Dalton Transactions

ROYAL SOCIETY OF CHEMISTRY

PAPER

View Article Online
View Journal | View Issue

Cite this: *Dalton Trans.*, 2022, **51**, 12604

Development of a series of flurbiprofen and zaltoprofen platinum(IV) complexes with anti-metastasis competence targeting COX-2, PD-L1 and DNA†

Zuojie Li,[a] Linming Li,[a,b] Wenhuan Zhao,[c] Bin Sun,[a] Zhifang Liu,[a] Min Liu,[a] Jun Han,[a] Zhengping Wang,[a,b] Dacheng Li[a,d] and Qingpeng Wang *[a]

Received 28th March 2022,
Accepted 26th July 2022

DOI: 10.1039/d2dt00944g

rsc.li/dalton

To develop new anti-metastasis chemotherapeutic drugs, a series of flurbiprofen (FLP) and zaltoprofen (ZTP) platinum(IV) complexes targeting COX-2, PD-L1 and DNA was prepared and investigated. Complex **2** with dual FLP ligands displays promising antitumor activities *in vitro* and exhibits much potential in overcoming drug resistance. More importantly, the antitumor evaluation *in vivo* demonstrates that complex **2** possesses promising inhibition of cancer growth and metastasis simultaneously. Further investigation of the mechanism revealed the multi-specific antitumor function of complex **2**. It exerts remarkable DNA damage after reduction to platinum(II) complex, and up-regulates the expression of p53 and γ-H2AX. Then, complex **2** promotes mitochondria-mediated apoptosis effectively by activating the Bcl-2/Bax/caspase3 pathway. Furthermore, inflammation in tumor tissues is restrained by the suppression of enzymes COX-2, MMP-9, NLRP3 and caspase1, which would favor the inhibition of tumor metastasis. Moreover, compound **2** boosts T-cell immunity by restraining PD-L1 expression, and further improving the density of $CD3^+$ and $CD8^+$ T cells in tumor tissues.

1. Introduction

Metastasis is a major cause of cancer morbidity and mortality, and accounts for about 90% of cancer deaths.[1,2] Despite the extensive efforts in cancer treatment, the overall survival (OS) of patients with metastatic cancer has not been significantly improved, because current predominant cancer treatments mainly focus on inhibition of cancer growth. Therefore, the development of novel effective chemotherapeutics with simultaneous inhibition of cancer growth and metastasis has become an important topic for researchers.[3,4]

Platinum-based chemotherapy as the first-line treatment for many cancers in the clinic exhibits striking therapeutic effects against the growth of primary tumors through causing serious DNA damage.[5] However, drawbacks such as toxicity, deactivation, drug resistance and tumor recurrence seriously hamper the outcomes in cancer treatment, especially in metastatic cancers.[6] Platinum(IV) compounds as prodrugs of platinum(II) drugs have been widely investigated in recent years and supply a new strategy to solve the problems above.[7,8] The octahedral configuration decreases deactivation of platinum(IV) complexes in blood and normal tissues in contrast to platinum(II) drugs, and further reduces toxicity. Moreover, the incorporation of various functional groups onto the axial ligands of the platinum(IV) scaffold affords a convenient way to overcome the drug resistance and tumor recurrence of traditional platinum(II) drugs.[9–12] Therefore, platinum(IV) complexes are of great potential to be developed as the next generation of platinum drugs.[7,13]

Inflammation in the tumor microenvironment (TME), as a hallmark of cancer, is closely associated with tumor growth, and plays an essential role in boosting the metastasis cascade of cancers.[14–18] A combination of inflammation inhibitory agent with platinum drug might produce promising metastasis inhibitory properties. NSAIDs including aspirin, ibuprofen, indomethacin and ketoprofen have been incorporated into the platinum(IV) system to form hybrids like **I–V** (Fig. 1) and have displayed effective antitumor activities by arousing significant inhibition of cyclooxygenases (COXs) to control the inflammatory response in tumor tissues besides causing serious DNA damage.[19–25]

[a]*Institute of Biopharmaceutical Research, Liaocheng University, Liaocheng 252059, P.R. China. E-mail: lywqp@126.com*
[b]*Liaocheng High-Tech Biotechnology Co., Ltd, Liaocheng 252059, P.R. China*
[c]*Frontier Biotechnologies Inc., Nanjing 210000, P.R. China*
[d]*Shandong Provincial Key Laboratory of Chemical Energy Storage and Novel Cell Technology, Liaocheng University, Liaocheng 252059, P.R. China*

†Electronic supplementary information (ESI) available: Detailed characterization data, ^1H and ^{13}C NMR spectra of new compounds. See DOI: https://doi.org/10.1039/d2dt00944g

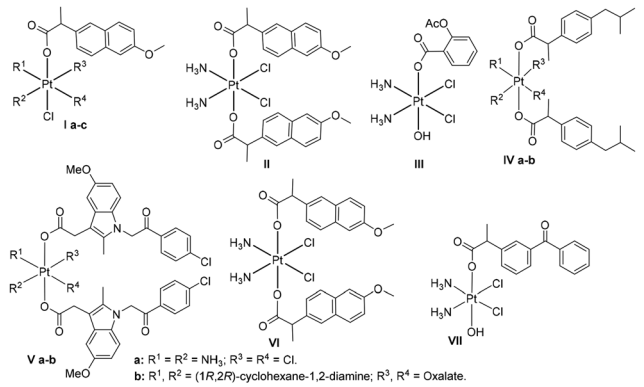

Fig. 1 Platinum(IV) complexes **I–VII** with NSAIDs ligands.

Immune suppression is another hallmark of cancer promoting tumor growth and metastases.[14] Blockade of immune check point programmed cell death-1 (PD-1)-programmed death ligand-1 (PD-L1) axis has opened up a new horizon in the cancer therapeutic landscape by modulating T-cell functions.[26–28] Recently, Guo's group and our group reported platinum(IV) complex **VI** and **VII** with naproxen and ketoprofen (KP) ligands as effective antitumor and anti-metastasis agents (Fig. 1), which could reverse immune suppression by down-regulating the expression of PD-L1 and restraining inflammation in TME.[20,29] With the aim of expanding the applications of NSAIDs platinum(IV) complexes in curing metastatic cancers, it is of great interest for us to investigate platinum(IV) complexes with other ligands, and further detect the likely mechanisms.

Flurbiprofen (FLP), as one of the most important COX inhibitors and NSAIDs, has been developed as an effective PD-L1 binder that has much potential in reversing immune suppression in cancer treatment.[30,31] Moreover, platinum(IV) conjugate **2** with FLP ligand was reported to show markedly higher cytotoxicity in cancer cells than cisplatin, FLP, and their physical mixture.[31] Yet, its antitumor mechanism has not been clarified. In addition, the combination of PD-L1 inhibitory drugs with platinum-based chemotherapy showed significantly increased therapeutic effects, and has emerged as a promising chemotherapeutic option especially in advanced cancers.[20,29,32] Inspired by the above conditions and as a constitution of our interest in developing novel antitumor platinum(IV) agents,[33–39] FLP was incorporated into the platinum (IV) system as a functional group targeting both COX and PD-L1 to form complexes **1–4** (Fig. 2), with the expectation that the target complexes would display prominent antiproliferative and anti-metastatic activities by modulating the inflammation and immune response in TME. Then, another NSAID, zaltoprofen (ZTP), as an analogue of FLP was also employed to generate complexes **5–9**. Classical platinum(II) drugs cisplatin and oxaliplatin were selected as cores of platinum(IV) complexes to investigate their influence on activities. Platinum(IV) complexes bearing dual and mono ligands were designed to determine the effects of ligands on their antitumor competence.

2. Results and discussion

2.1 Chemistry

Platinum(IV) complexes **1–9** with FLP and ZTP ligands were synthesized with commercially available cisplatin, oxaliplatin, FLP and ZTP as starting materials. The oxidation of cisplatin

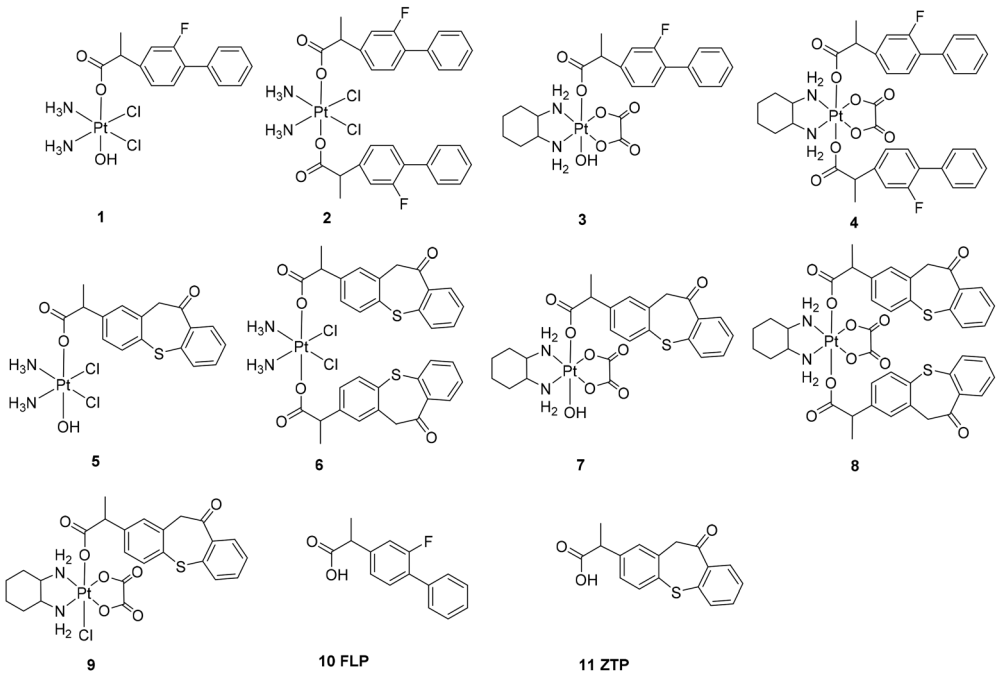

Fig. 2 Structure of FLP and ZTP platinum(IV) complexes **1–9**.

and oxaliplatin with hydrogen peroxide or *N*-chlorosuccinimide (NCS) afforded the corresponding oxoplatins **O1–O3** (Scheme S1†). Then, the condensation of oxoplatins **O1–O3** with 1.1 equivalents of FLP or ZTP in the presence of *N,N,N′,N′*-tetramethyl-*O*-(benzotriazol-1-yl)uronium tetrafluoroborate (TBTU) and *N,N,N*-triethylamine (TEA) produced the mono FLP and ZTP platinum(IV) complexes **1**, **3**, **5**, **7** and **9** in yields of 22–32%. Meanwhile, the dual FLP and ZTP platinum(IV) complexes **2**, **4**, **6** and **8** were prepared by the reaction of oxoplatins **O1–O2** with 2.5 equivalents of FLP or ZTP in yields of 27–42%.

2.2 Antitumor activities *in vitro*

The antiproliferative activities of platinum(IV) complexes **1–9** with FLP and ZTP ligands were determined using a MTT assay with cisplatin, oxaliplatin, FLP (**10**) and ZTP (**11**) as reference drugs. Six tumor cell lines including human ovarian cancer (SKOV-3), human lung cancer (A549), cisplatin-resistant human lung cancer (A549R), human liver cancer (HepG2), murine breast cancer (4T1) and murine colon cancer (CT-26), and one human normal liver cell line (LO2) were evaluated and the results were given as IC_{50} values based on three parallel experiments.

Results in Table 1 reveal that complexes **1–8** display moderate to effective antitumor activities *in vitro*; meanwhile, platinum(IV) compound **9** with chloride ligand shows weak cytotoxic effects on tumor cells. The platinum core exerts great impacts on the activities, and cisplatin-derived platinum(IV) complexes **1**, **2**, **5** and **6** lead to relatively more outstanding antiproliferative competence than the corresponding oxaliplatin ones **3**, **4**, **7** and **8**. Moreover, the FLP platinum(IV) conjugates **1–4** are relatively more effective than the corresponding ZTP platinum(IV) hybrids **5–8**. Especially complexes **1** and **2** afford IC_{50} values lower than 1.64 μM toward all tested tumor cell lines. As for the mono ligand complexes and dual ligand ones, the FLP and ZTP conjugates exhibit rather different trends. Dual FLP platinum(IV) hybrids **2** and **4** are significantly more effective than the mono FLP ones **1** and **3**. Meanwhile, the mono ZTP platinum(IV) complexes **5** and **7** are more promising than the dual ZTP ones **6** and **8**. Notably, complex **2** shows the most effective activities among the tested complexes, with low IC_{50} values in nanomolar degree in all tested tumor cell lines (IC_{50} < 0.29 μM), which are more effective than cisplatin and oxaliplatin.

To determine the potency of the title compounds in defeating the resistance of cisplatin, the resistant factor (RF) as a ratio of IC_{50} value of A549R to that of A549 was calculated. Complexes **1** and **2** with FLP ligand lead to lower RF values of 0.48 and 0.34 than the ZTP-modified ones **5** and **6** (RF = 0.53 and 1.13), which are superior to cisplatin (RF = 3.10). These results indicate their potency in overcoming the resistance of cisplatin.

Then a normal cell line LO2 was tested to evaluate the toxic properties of the tested complexes. Tumor selectivity index (SI), defined as a ratio of IC_{50} for normal liver cell LO2 to IC_{50} value of liver cancer HepG2, was calculated to determine the tumor-selective potential of the tested complexes. It was observed that platinum(IV) complex **1**, **2** and **5** exerted promising tumor selectivity with high SI values of 4.68, 3.51 and 7.33, which are higher than cisplatin and oxaliplatin (SI = 0.85, 0.79), indicating their potential in improving tumor selectivity.

Accordingly, the FLP and ZTP platinum(IV) complexes, especially complexes **1**, **2**, **5** and **6** with cisplatin core, display potent antitumor activities *in vitro*, and show great potential in defeating cisplatin resistance and reducing toxicity. Thereby, complexes **1**, **2**, **5** and **6** were further evaluated for antitumor activities *in vivo*.

2.3 Antitumor activities *in vivo*

The antitumor activities *in vivo* against CT-26 homograft tumors were tested on male BALB/c mice. Complexes **1**, **2**, **5** and **6** were administered at a dosage of 4 mg Pt per kg (i.p.) for 4 times on days 3, 6, 9 and 12 with clinical platinum(II) drugs cisplatin and oxaliplatin as reference drugs (Fig. S1a†). A saline group was set as blank. The results reveal that all the tested platinum(IV) complexes **1**, **2**, **5** and **6** possess reduced

Table 1 Cytotoxicity profiles of FLP and ZTP platinum(IV) complexes toward six carcinoma cell lines and one normal cell line after 48 h treatment expressed as IC_{50} (μM)

Compd.	SKOV-3	A549	A549R	RF[a]	4T1	CT26	HepG2	LO2	SI[b]
1	0.32 ± 0.06	1.64 ± 0.09	0.80 ± 0.30	0.48	1.51 ± 0.09	0.56 ± 0.21	0.34 ± 0.07	1.59 ± 0.19	4.68
2	0.11 ± 0.02	0.29 ± 0.01	0.10 ± 0.01	0.34	0.14 ± 0.02	0.21 ± 0.04	0.05 ± 0.01	0.19 ± 0.04	3.51
3	25.38 ± 3.95	48.34 ± 0.62	14.72 ± 2.51	0.30	15.49 ± 1.20	17.61 ± 2.21	14.53 ± 2.63	24.30 ± 2.85	1.67
4	1.77 ± 0.67	10.74 ± 8.66	3.70 ± 1.06	0.34	5.17 ± 1.63	6.38 ± 0.49	2.27 ± 0.35	3.71 ± 0.65	3.71
5	0.13 ± 0.05	0.39 ± 0.05	0.21 ± 0.05	0.53	0.58 ± 0.11	0.24 ± 0.11	0.92 ± 0.26	0.78 ± 0.18	0.85
6	3.82 ± 1.48	4.98 ± 0.84	5.64 ± 0.86	1.13	6.15 ± 1.61	6.94 ± 0.77	1.12 ± 0.19	8.20 ± 1.02	7.33
7	1.30 ± 0.41	5.71 ± 2.54	6.27 ± 2.58	1.10	5.17 ± 1.19	9.28 ± 1.52	5.24 ± 0.66	3.83 ± 0.24	0.73
8	2.27 ± 0.16	6.91 ± 1.78	11.18 ± 2.82	1.62	17.55 ± 5.50	7.93 ± 1.66	18.21 ± 3.47	34.45 ± 4.51	1.89
9	>50	>50	>50	ND[c]	ND	ND	3.13 ± 0.46	ND	ND
10	>50	>50	>50	ND	>50	>50	ND	ND	ND
11	>50	>50	>50	ND	>50	>50	ND	ND	ND
Cisplatin	0.71 ± 0.05	5.18 ± 0.45	16.05 ± 2.40	3.10	4.62 ± 0.95	1.84 ± 0.28	3.26 ± 0.45	2.78 ± 0.10	0.85
Oxaliplatin	0.66 ± 0.14	9.68 ± 1.72	4.19 ± 0.43	0.43	13.29 ± 4.42	4.70 ± 0.41	4.71 ± 0.32	3.72 ± 0.24	0.79

[a] RF: resistant factor, RF = IC_{50}(A549R)/IC_{50}(A549) [b] SI: selectivity index, SI = IC_{50}(LO2)/IC_{50}(HepG2) [c] ND: not tested or not calculated.

toxicity in comparison with the platinum(II) reference drugs cisplatin and oxaliplatin at the same dosage. Cisplatin induced a dramatic decrease of body weight on day 8 after twice administration (Fig. 3a), and the survival rate decreased to 16.7% on day 9 (Fig. S1b†), which indicates the serious toxicity of cisplatin. Meanwhile, oxaliplatin also caused significant body weight loss of 13.7% at the end of the experiment (day 17). Encouragingly, all tested platinum(IV) complexes did not decrease the survival rate of mice, and exerted lower influence on body weight than cisplatin and oxaliplatin. Complexes **1**, **2** and **5** caused no obvious impact on body weight in contrast to the saline group (P = ns), and are superior to complex **6**. Furthermore, the hematoxylin and eosin (H&E) staining of liver, spleen and kidney tissue in Fig. S3† also shows that the administration of platinum(IV) complexes **1**, **2**, **5** and **6** causes no appreciable histological differences in organs in comparison with the saline group. As revealed in the literature, hepatotoxicity and nephrotoxicity have emerged as major factors limiting the therapeutic usefulness of platinum drugs.[40] Thereby, aspartate aminotransferase (AST) and alanine aminotransferase (ALT) in serum, associated with hepatotoxicity, and blood urea nitrogen (BUN) and creatinine (CRE), associated with nephrotoxicity, were evaluated by enzyme-linked immunosorbent assay (ELISA). Results in Fig. 3e demonstrate that all platinum(IV) complexes **1**, **2**, **5** and **6** induced no significant change of ALT, AST, BUN and CRE levels in serum compared with the blank group, which further verified their weak toxicities in liver and kidneys.

The antitumor efficacies were analysed by monitoring tumor volume during the experiment, and measuring the tumor weight at the end of the experiment. Complexes **1**, **2** and **6** significantly suppressed the volumes of tumors to V < 287 mm^3, which were significantly smaller than in the saline group (831 mm^3, P < 0.001). Meanwhile, complex **5** exerted a relatively lower inhibition on tumor growth (528 mm^3). Then, tumor growth inhibit rate (TGI) as a rate of tumor weight of the drug-treated group to the tumor weight of the saline group was calculated. FLP complex **1** and **2** possessed superior antitumor performances with TGI values of 32.5% and 70.8% in contrast to the corresponding ZTP complexes **5** and **6** (TGI = 25.7%, 44.5%). Especially, dual FLP platinum(IV) complex **2** exerted the most promising antitumor activities among the tested complexes, offering a higher TGI value than oxaliplatin (TGI = 57.8%). Apoptosis of tumor cells was observed in the H&E staining of tumor tissues for complex **2** (Fig. S4†).

A direct comparison with the results reported in our previous work[29] about the KP platinum(IV) complexes revealed that dual FLP platinum(IV) complex **2** exhibits relatively more

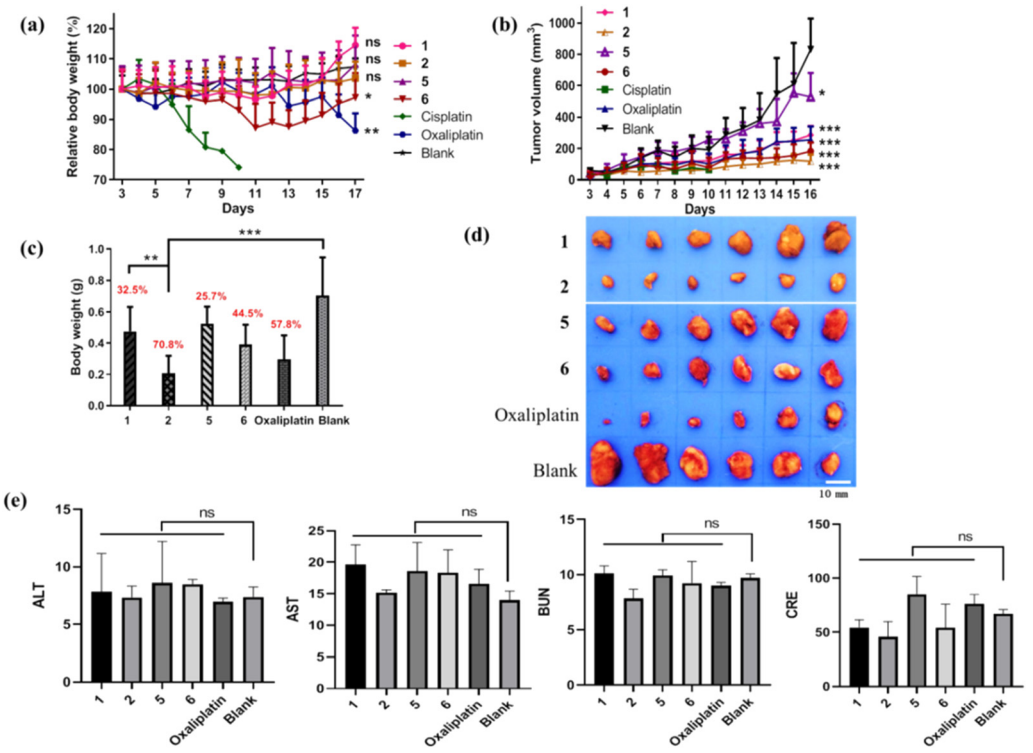

Fig. 3 *In vivo* antitumor activities of compounds **1**, **2**, **5**, **6**, cisplatin and oxaliplatin to CT-26 tumors in BALB/c mice (n = 6). *P < 0.05, **P < 0.01, ***P < 0.001, ns: no significant difference compared with control group. (a) Relative body weight of the mice during the treatment. (b) Tumor growth as a function of time. (c) Tumor weight of each group at the end of the experiment. The TGI values of the tested drugs in comparison with saline group are depicted in red above the column (TGI = tumor weight of drug treated group/tumor weight of saline group × 100%). (d) Image of tumors at the end of the experiment. Reprinted with permission from Li *et al.*, *J. Med. Chem.*, 2021, **64**, 17920. Copyright 2021 American Chemical Society.[29] (e) Serum ALT, AST, BUN and CRE levels in mice.

significant tumor growth inhibition (TGI = 70.8%) than the mono KP ligand complex **VII** (TGI = 57.1%). Notably, the FLP and KP platinum(IV) complexes show rather different trends in displaying antitumor activities. The dual FLP platinum(IV) complex **2** exhibits more promising antitumor competence *in vivo* than the mono ligand one **1** (Fig. S1e†); meanwhile, mono KP platinum(IV) complex **VII**[29] is more potent than the corresponding complex with dual KP ligands, which indicates that different ligand incorporated into the platinum(IV) system leads to rather different effects on the antitumor performance of the target complexes.

To further verify the antitumor competences of FLP platinum(IV) complex *in vivo*, the activities of **1** and **2** (4 mg Pt per kg) against 4T1 tumors in female BALB/c mice were also tested, with cisplatin (2 mg Pt per kg) and oxaliplatin (4 mg Pt per kg) as reference drugs. Results in Fig. 4 reflect that complex **2** exhibited prominent tumor growth inhibition to 4T1 tumors with higher TGI of 63.9% than complex **1** (TGI = 49.4%), which is similar to cisplatin and oxaliplatin (TGI = 57.1% and 62.5%) as well as KP platinum(IV) complex **VII**[29] (TGI = 54.6%) (Fig. S2†). This trend is mainly in accordance with the CT-26 test *in vivo*, and provides further evidence of the prominent antitumor competence of compound **2**.

Drug accumulation in tumor tissues is a key index affecting the antitumor properties of metallic drugs. Thus the platination level of complexes **1**, **2** and oxaliplatin in CT-26 tumors was measured by ICP-MS. Results in Fig. S5† indicate that both FLP platinum(IV) complexes **1** and **2** afford an increased drug accumulation level in tumors in comparison with the platinum(II) drug oxaliplatin ($P < 0.001$). However, the platination of dual FLP platinum(IV) complex **2** with the most prominent antitumor activities *in vivo* is relatively lower than the mono FLP hybrid **1**, which demonstrates that the accumulation level in tumors is an important but not the only factor influencing the antitumor activities *in vivo*.

2.4 Metastasis inhibition *in vitro* and *in vivo*

Metastasis is the main factor causing mortality in cancer patients. To further extend the application of FLP platinum(IV) complexes in the treatment of metastatic cancers, the metastasis inhibitory properties of complexes **1** and **2** were tested *in vivo* with cisplatin and oxaliplatin as reference drugs.

Lung is one of the most common sites for tumor metastasis.[41] In this experiment, pulmonary metastasis models were established by injection of 4T1 cells (2×10^5 cells per mouse) *via* the tail vein to evaluate their effectiveness against pulmonary metastasis *in vivo* (Fig. S6†). Encouragingly, complexes **1** and **2** successfully reduced the number of lung metastasis nodules to 26.8% and 13.7% of the blank group, which is remarkably more potent than cisplatin (34.5%, $P < 0.001$) and oxaliplatin (59.3%, $P < 0.001$) (Fig. 5). Especially, complex **2**, with the most promising antitumor competence *in vivo*, also exhibits the best metastatic inhibition ability, which is over 2.5- and 4.3-fold more potent than cisplatin and oxaliplatin. These results were also verified by the H&E staining images of lung tissues: the complex **2**-treated group afforded fewer and smaller nodules in the lung than cisplatin and oxaliplatin. Notably, the potent pulmonary metastasis inhibitory properties of complex **2** (13.7%) are similar to that of the KP platinum(IV) compound **VII** (15.9%) (Fig. S6†),[29] and these facts synergistically demonstrate the great potential of NSAID platinum(IV) complexes as anti-metastasis agents.

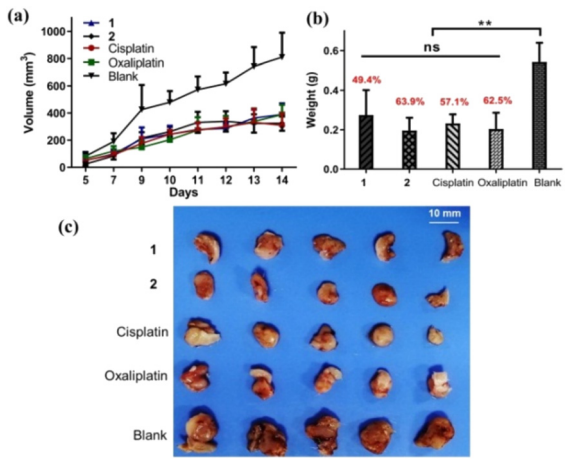

Fig. 4 *In vivo* antitumor activities of compounds **1**, **2**, cisplatin and oxaliplatin to 4T1 tumors in BALB/c mice ($n = 5$). Drugs (**1**, **2**, oxaliplatin: 4 mg Pt per kg; cisplatin: 2 mg Pt per kg) were administered on days 3, 6, 9 and 12, and the mice were sacrificed on day 15. *$P < 0.05$, **$P < 0.01$, ***$P < 0.001$, ns: no significant difference compared with control group. (a) Tumor growth as a function of time. (b) Tumor weight of each group at the end of the experiment. The TGI values of the tested drugs in comparison with saline group are depicted in red above the column. (c) Image of tumors at the end of the experiment. Reprinted with permission from Li *et al.*, *J. Med. Chem.*, 2021, **64**, 17920. Copyright 2021 American Chemical Society.[29]

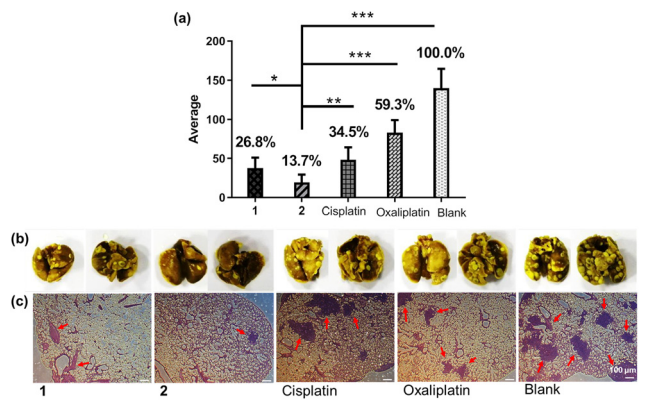

Fig. 5 Pulmonary metastasis inhibition of compounds **1**, **2**, cisplatin and oxaliplatin against 4T1 breast carcinoma tumors *in vivo* ($n = 5$). *$P < 0.05$, **$P < 0.01$, ***$P < 0.001$, ns: no significant difference compared with control group. (a) Lung nodules in each group. (b) Representative photographs of front and back sides of lungs from each group at the end of the experiment. (c) H&E staining of lung metastasis nodules. Nodules are indicated by red arrows. Reprinted with permission from Li *et al.*, *J. Med. Chem.*, 2021, **64**, 17920. Copyright 2021 American Chemical Society.[29]

The anti-metastatic potency of complex **2** was also evaluated by transwell assay and wound-healing assay *in vitro*. Results in Fig. 6 reflect the strong migration inhibition of platinum(IV) conjugate **2** *in vitro*; it significantly decreased the relative migration rate to 6.8% at concentration of 2 μM, which is remarkably lower than cisplatin at the same concentration (65.4%, $P < 0.001$) as well as oxaliplatin at a higher concentration of 10 μM (19.9%, $P < 0.001$). Meanwhile, the wound-healing results in Fig. S7† provide further evidence of the prominent migration inhibition of complex **2** to tumor cells than cisplatin and oxaliplatin *in vitro*. The mechanisms of action were then investigated in the following experiments from multiple aspects.

2.5 Stability and DNA damage

The stability of dual FLP platinum(IV) complex **2** was evaluated in PBS and biological media RPMI1640 at 37 °C. The HPLC results in Fig. S8† reflect that complex **2** remains stable for at least 24 h in biological media PBS and RPMI1640. To further evaluate its stability in blood, the half life of complex **2** in whole blood of mice was measured (Fig. S9†). Complex **2** shows a longer half life in blood ($t_{1/2}$ = 3.9 h) than those reported for cisplatin ($t_{1/2}$ = 21.6 min) and satraplatin ($t_{1/2}$ = 6 min),[42] reflecting its elevated stability *in vivo*. The dual KP platinum(IV) complex reported in our previous work was proved to be poorly stable in normal biological media,[29] which further restrained its antitumor activities *in vivo*. And these facts might be the reasons accounting for the distinct trends of FLP and KP platinum(IV) complexes in displaying antitumor activities. Taking the promising stability of complex **2** in biological media and its longer half-life in blood into consideration, it is reasonable to deduce that complex **2** enters tumor cells as an intact lipophilic molecule and exerts a distinct antitumor mechanism with platinum(II) drug cisplatin, which is similar to that of the mono KP platinum(IV) complexes **VII**.[29]

DNA is the main target of platinum drugs. Platinum(IV) complexes were expected to undergo reduction in reducing TME to release platinum(II) complexes and further induce serious DNA damage to cause apoptosis of tumor cells. The reduction property of complex **2** was evaluated in the presence of biological reductant AsA, and the DNA damage competence was further tested with 5′-GMP as a model of DNA base. Moreover, proteins p53 and γ-H2AX, as indicators of DNA injury in cells, were measured by western blot assay. Complex **2** easily undergoes reduction in the presence of AsA (1 mM, same concentration as in TME) (Fig. S8†). Furthermore, the released platinum(II) complex would conjoin with 5′-GMP to form Pt-GMP adduct, which demonstrates the DNA binding potency of the platinum(IV) complex. The DNA damage caused by complex **2** was also verified by the significant up-regulated expression of p53 and γ-H2AX ($P < 0.001$) (Fig. 7).

2.6 Apoptosis induction

The ability of platinum(IV) complexes to induce apoptosis of tumor cells was examined using an Annexin V-FITC/PI double staining assay. Results in Fig. 8 show that all tested complexes **1**, **2**, **5** and **6** are effective in causing apoptosis. Notably, complex **2** leads to a high portion of cells (57.2%) undergoing apoptosis at a lower concentration of 5 μM, which is comparable to that of the reference drugs cisplatin (67.2%) and oxali-

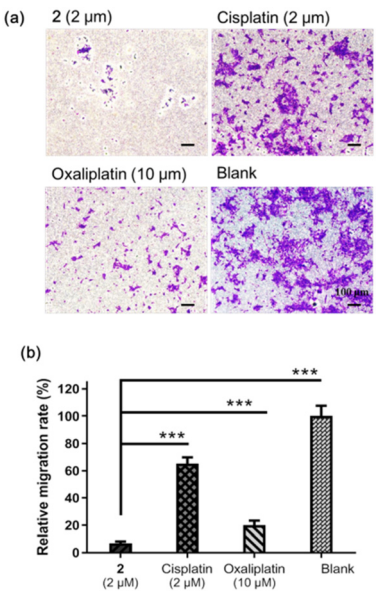

Fig. 6 Evaluation of migration inhibition properties of complex **2** (2 μM), cisplatin (2 μM) and oxaliplatin (10 μM) to 4T1 cells using transwell assay *in vitro*. The tumor cells were treated with and without platinum complexes for 24 h. (a) Representative images. (b) Analysis of relative migration rate. *$P < 0.05$, **$P < 0.01$, ***$P < 0.001$, ns: no significant difference compared with control group.

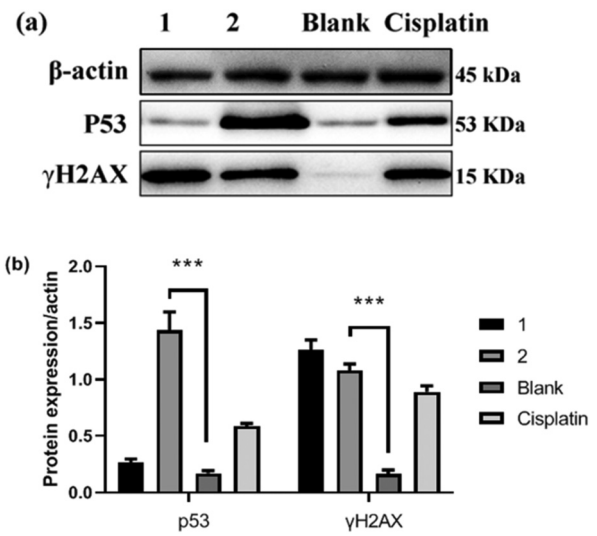

Fig. 7 Western blot analysis of p53 and γ-H2AX expression. A549 cells were incubated with and without platinum compounds **1**, **2** and cisplatin (10 μM) for 24 h at 37 °C. (a) Blots. (b) Relative gray intensity analysis (relative gray intensity = gray intensity of indicated protein/gray intensity of β-actin). *$P < 0.05$, **$P < 0.01$, ***$P < 0.001$, ns: no significant difference compared with control group.

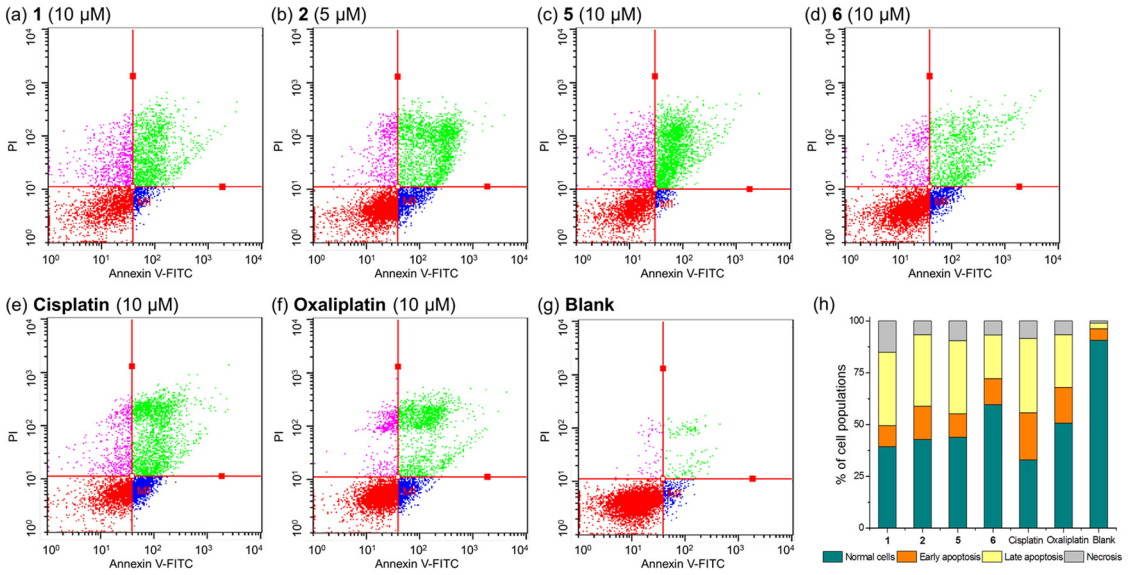

Fig. 8 Apoptosis inducing properties of complexes **1**, **2**, **5**, **6**, cisplatin and oxaliplatin in A549 cells. A549 cells were incubated with and without platinum complexes for 24 h at 37 °C, and evaluated using an annexin V-FITC/PI double staining assay. (a) **1** (10 μM). (b) **2** (5 μM). (c) **5** (10 μM). (d) **6** (10 μM). (e) Cisplatin (10 μM). (f) Oxaliplatin (10 μM). (g) Blank. (h) The stacking columns.

platin (49.3%) at a higher concentration of 10 μM. These facts reflect the promising ability of complex **2** in inducing apoptosis.

2.7 Mitochondrial apoptotic pathway

Mitochondria, as the main energy production site, display a great role in regulating apoptosis of tumor cells. Depolarization of the mitochondrial membrane as an early indicator of mitochondrial dysfunction is related to the production of ROS, which serves as an important factor in activating the mitochondrial apoptotic pathway. To determine whether these platinum(IV) complexes could disturb the function of mitochondria, the mitochondrial membrane potential ($\Delta\Psi_m$) change and ROS generation were measured using the fluorescent probes JC-1 and DCFH-DA, respectively, after treating A549 cells with different drugs for 24 h. The proteins Bcl-2, Bax, caspase3 and *c*-caspase3 involved in mitochondrion-mediated apoptosis were evaluated by western blot assay.

It was shown that platinum(IV) complexes **1**, **2**, **5** and **6** are potent in causing loss of $\Delta\Psi_m$ (Fig. 9). Complex **2** leads to the most remarkable decrease of $\Delta\Psi_m$ (81.48%) even at a low concentration of 5 μM, which is superior to that of cisplatin and oxaliplatin as well as complexes **1**, **5** and **6** at 10 μM. Subsequently, the ROS generation detection shown in Fig. 10 reflects that complex **2** (5 μM) also leads to obviously higher ROS accumulation in tumor cells than cisplatin, oxaliplatin and complex **1** (10 μM). The trends for the $\Delta\Psi_m$ loss and ROS production are mainly in accordance with the antitumor activities *in vitro*.

As depicted in Fig. 11, the expression of apoptosis-antagonizing protein Bcl-2 is significantly down-regulated after incubation with FLP platinum(IV) complexes **1** and **2** for 24 h; meanwhile, the pro-apoptosis protein Bax is up-regulated. Then, the overexpression of effector protein caspase3 and *c*-caspase3 was observed. Accordingly, the FLP platinum(IV) complexes could promote apoptosis of tumor cells through the intrinsic mitochondrial pathway Bcl-2/Bax/caspase3.

2.8 Inflammation inhibition

Tumor-recruited inflammation is an important hallmark of cancer, and plays a pivotal role in tumor initiation, progression and metastasis through different pathways. COX-2 as the main target of NSAIDs has been heralded as a promising target for cancer therapy. Another crucial enzyme, matrix metalloproteinase-9 (MMP-9) in TME, which is capable of degrading basement membrane, plays a synergistic function with COX-2 in promoting tumor inflammation and metastasis. In addition, inflammasome NLRP3 as a multi-protein is responsible for the processing of caspase1. The activation of the NLRP3/caspase1 pathway has been proved to be closely associated with various inflammatory diseases.[43,44] Thereby, the influence of FLP platinum(IV) complexes **1** and **2** on the expression of COX-2, MMP-9, NLRP3 and caspase1 in tumor cells was detected.

The western blots in Fig. 12 reveal that complex **2** significantly reduced COX-2 and MMP-9 to 2.6% and 39.3% of blank group; NLRP3 and caspase1 were also down-regulated by compound **2** to 45.0% and 49.0%, respectively. Meanwhile, mono FLP platinum(IV) hybrid **1** exhibits relatively lower influence on the tested proteins than dual FLP complex **2**. The inflammation inhibitory properties of complexes **1** and **2** *in vivo* were also confirmed by the immunohistochemical staining of COX-2 and MMP-9 in tumor tissues. Micrographs in Fig. 13 depict that COX-2 and MMP-9 in tumor tissues were obviously down-regulated by the FLP platinum(IV) complexes **1** and **2**,

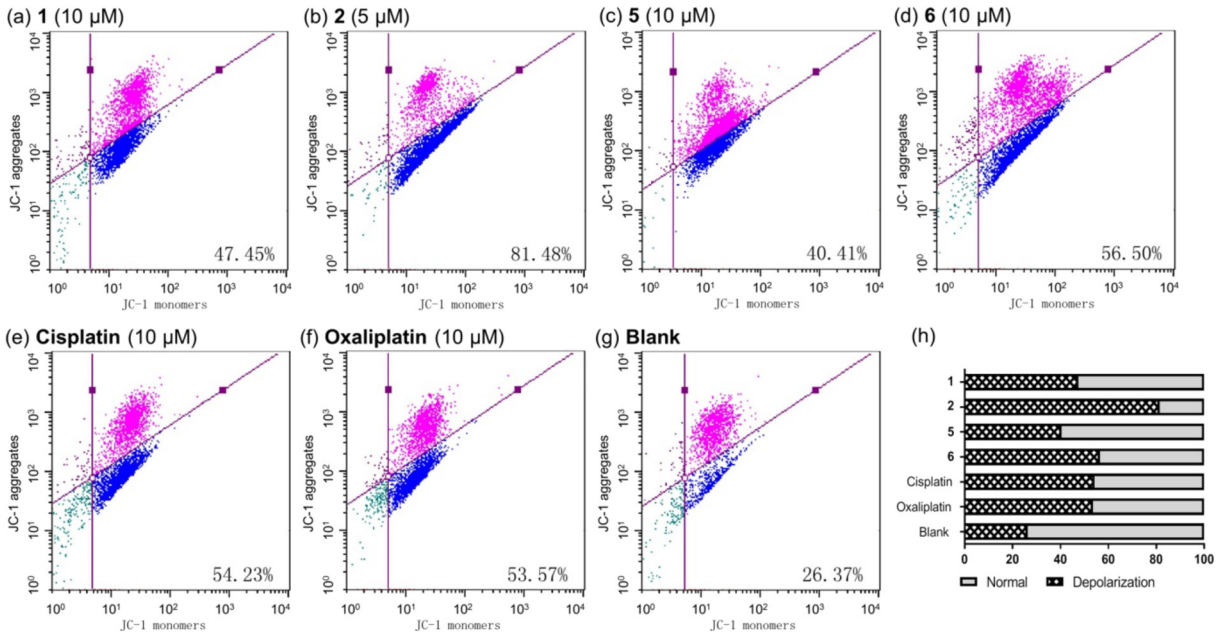

Fig. 9 Mitochondrial membrane potential ($\Delta\Psi_m$) analyzed by flow cytometry. A549 cells were treated with and without platinum complexes for 24 h at 37 °C, and stained with JC-1. (a) **1** (10 μM). (b) **2** (5 μM). (c) **5** (10 μM). (d) **6** (10 μM). (e) Cisplatin (10 μM). (f) Oxaliplatin (10 μM). (g) Blank. (h) Statistical analysis of the decrease of $\Delta\Psi_m$.

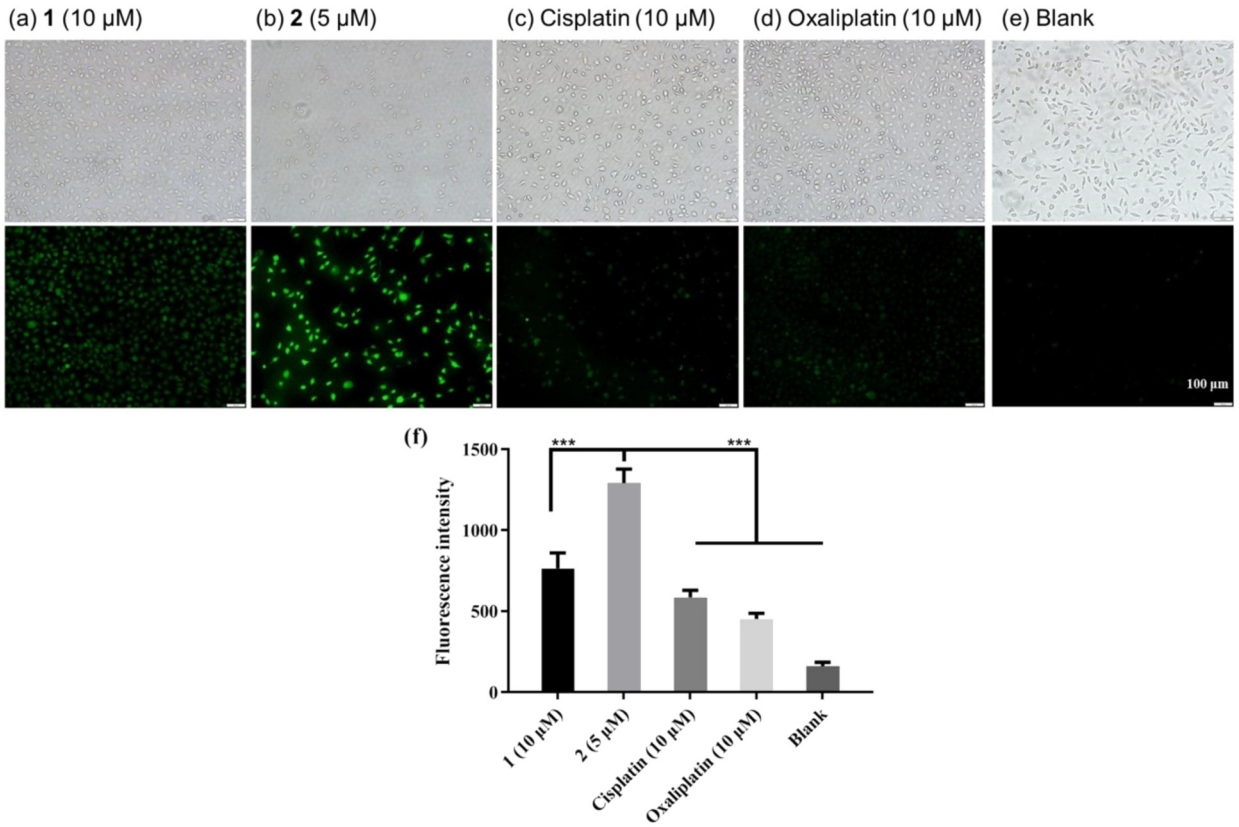

Fig. 10 Staining of ROS with DCFH-DA in A549 cells treated by platinum complexes for 24 h at 37 °C. (a) **1** (10 μM). (b) **2** (5 μM). (c) Cisplatin (10 μM). (d) Oxaliplatin (10 μM). (e) Blank. (f) Statistical analysis of fluorescence intensity by flow cytometry. *P < 0.05, **P < 0.01, ***P < 0.001, ns: no significant difference compared with blank group.

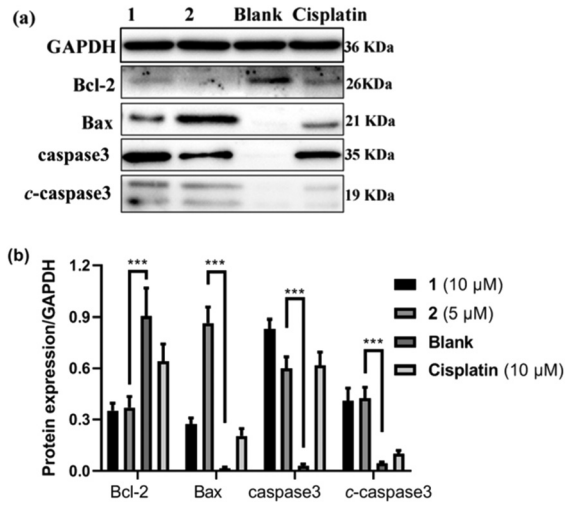

Fig. 11 Expression of Bcl-2, Bax, caspase3 and *c*-caspase3 in A549 cells after treatment with complex **1** (10 μM), **2** (5 μM) and cisplatin (10 μM) for 24 h. The untreated group was set as blank. (a) Blots. (b) The ratios of proteins to GAPDH. *$P < 0.05$, **$P < 0.01$, ***$P < 0.001$, ns: no significant difference compared with blank group.

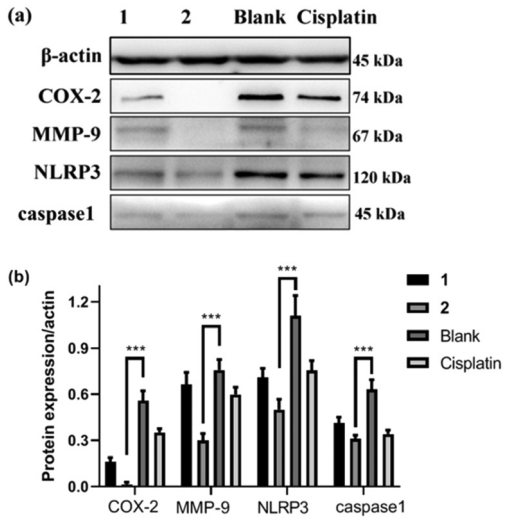

Fig. 12 Expressions of COX-2, MMP-9, NLRP3 and caspase1 in A549 cells after treatment with complex **1** (10 μM), **2** (5 μM) and cisplatin (10 μM) for 24 h. The untreated group was set as blank. (a) Blots. (b) The ratios of proteins to β-actin. *$P < 0.05$, **$P < 0.01$, ***$P < 0.001$, ns: no significant difference compared with blank group.

while oxaliplatin even leads to increased expression of COX-2 and MMP-9, indicating its negative impacts on inflammation inhibition. In summary, platinum(IV) complexes with FLP ligands, especially complex **2**, are of great potential in reducing tumor-related inflammation through the suppression of key enzymes COX-2, MMP-9, NLRP3 and caspase1.

2.9 Immune modulation

Immune suppression in TME is crucial for the development and metastasis of tumors.[45] Immune checkpoint PD-L1 plays a crucial role in facilitating tumor immune evasion and serves as a promising target for antitumor immunotherapy.[46,47] Moreover, there is compelling evidence that high expression of COX-2 could promote immune escape of tumor cells through the PD-L1 pathway.[48,49] Additionally, FLP was recognized as a PD-L1 binder in previous work.[30] Thereby, FLP platinum(IV) complexes possessing potent COX-2 inhibition are expected to down-regulate the expression of PD-L1, activate the immune response in TME, and inhibit the growth and metastasis of tumors.

Herein, the expression of PD-L1 in tumor tissues was detected by immunohistochemistry. Results in Fig. 14 demonstrate that the candidate compound dual FLP platinum(IV) complex **2** exhibits remarkable suppression of PD-L1 to 13.2% of the blank group in tumor tissues, which is relatively superior to that of the mono FLP compound **1** (33.3%, $P < 0.01$) and oxaliplatin (132.5%, $P < 0.001$). Moreover, it has been demonstrated that the blockade of immune checkpoint PD-L1 would activate tumor-infiltrating lymphocytes (TILs) to eliminate the immune suppression and restore immune system function.[27,28,50] Therefore, the $CD3^+$ and $CD8^+$ T cells in tumor tissues were stained by immunohistochemistry. It was found that the density of $CD3^+$ and $CD8^+$ T cells in tumor tissues treated with complexes **1** and **2** was raised significantly in comparison with the saline group ($P < 0.001$). These results provide evidence for the fact that the FLP platinum(IV) complexes could boost T-cell immunity in TME by restraining PD-L1 expression, and further improve the density of $CD3^+$ and $CD8^+$ T cells. The potent immunomodulatory effects exert significant influences on tumor proliferation and metastasis.

3. Experimental

3.1 Chemistry

3.1.1 General. All the reagents and solvents were of analytical grade and used without further purification. The platinum drugs cisplatin and oxaliplatin were purchased from Boyuan Pharmaceutical Co., Ltd (Jinan, China), and other reagents were obtained from Aladdin (Shanghai, China), Innochem Company (Beijing, China), Sigma and J&K. All reactions were carried out under an atmosphere of nitrogen in flame-dried glassware with magnetic stirring unless otherwise indicated. The ^{1}H-NMR and ^{13}C-NMR spectra were recorded on a Bruker spectrometer (500 MHz and 126 MHz) in DMSO-d_6 with residual solvent peaks or TMS as an internal standard. All coupling constants J were quoted in Hz. The MS spectra were obtained on a mass spectrometer with ESI ionization (Shimadzu LC-MS/MS 8040). Flow cytometry was performed on a Millipore Guava easyCyte 8HT flow cytometer. The HPLC analyses were carried out on a Thermo Ultimate 3000 RS equipped with an Agilent Eclipse XDB-C18 column (250 × 4.6 mm, 5 μm).

3.1.2 Synthetic procedure. The synthetic procedures for oxoplatins **O1–O3** are given in the ESI† according to procedures reported in our previous work.[36,37]

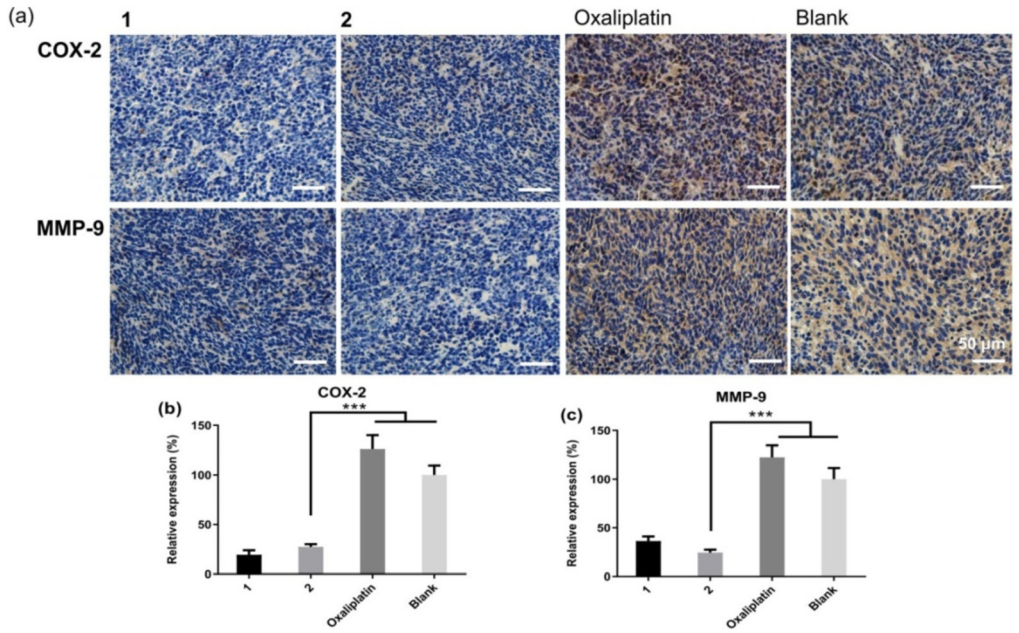

Fig. 13 Immunohistochemical staining of COX-2 and MMP-9 in tumor tissues from BALB/c mice bearing CT-26 homograft tumors. (a) Representative micrographs. (b) Quantified data of COX-2 expression. (c) Quantified data of MMP-9 expression. *$P < 0.05$, **$P < 0.01$, ***$P < 0.001$, ns: no significant difference compared with blank group.

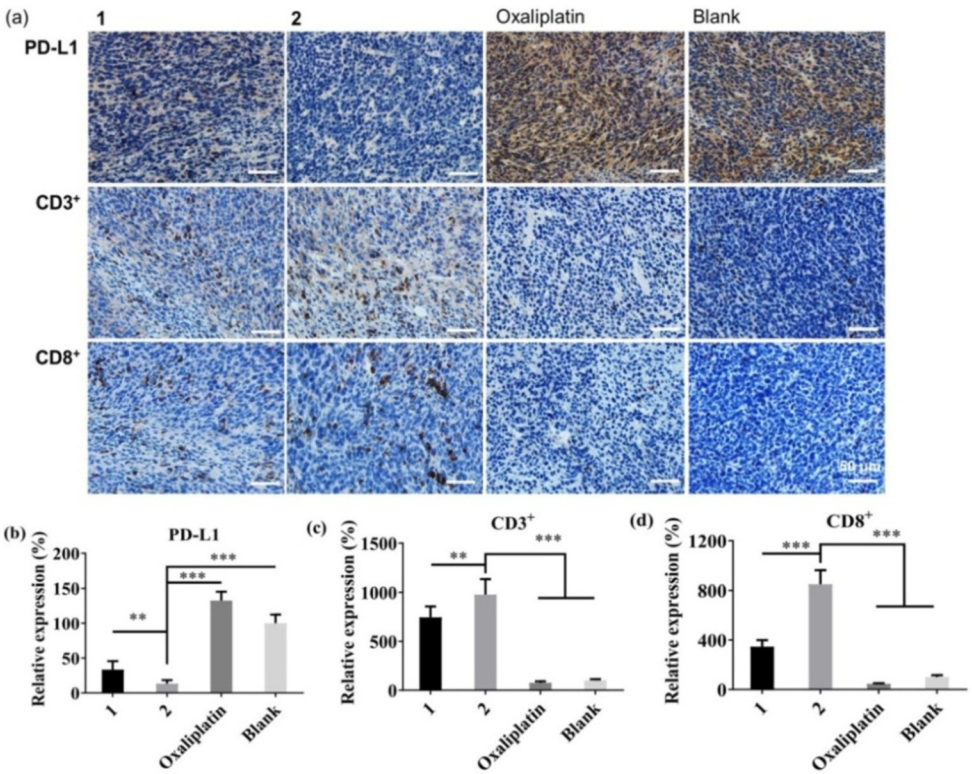

Fig. 14 Immunohistochemical staining of PD-L1, $CD3^+$ and $CD8^+$ in tumor tissues from BALB/c mice bearing CT-26 homograft tumors after treatment by each complex. (a) Representative micrographs. (b) Quantified data of PD-L1 expression. (c) Quantified analysis of $CD3^+$ T cells. (d) Quantified analysis of $CD8^+$ T cells. *$P < 0.05$, **$P < 0.01$, ***$P < 0.001$, ns: no significant difference compared with blank group.

*3.1.2.1 Preparation of compound **1**.* To a solution of FLP **10** (54 mg, 0.22 mmol) and TBTU (71 mg, 0.22 mmol) in dry DMF 5 mL was added TEA (30 μL, 0.22 mmol) and stirred for 10 min at room temperature. Then, oxoplatin **O1** (66 mg, 0.20 mmol) was added to the solution, and the mixture was further stirred for 48 h at 50 °C in the dark. After that, the solvent was removed under vacuum. The residue was subsequently purified by silica gel column chromatography. Subsequently, pure complex **1** was obtained as a pale solid (33.5 mg, 30%).

^{1}H NMR (500 MHz, DMSO-d_6) δ 7.55–7.51 (m, 2H), 7.47 (t, J = 7.8 Hz, 2H), 7.43–7.36 (m, 2H), 7.31–7.21 (m, 2H), 6.31–5.44 (m, 6H, NH_3), 3.70 (q, J = 7.1 Hz, 1H), 1.48–1.26 (m, 3H). ^{13}C NMR (126 MHz, DMSO-d_6) δ 181.70, 160.24, 158.30, 145.57, 135.67, 130.53, 129.16, 129.05, 128.08, 126.30, 124.72, 115.79, 115.61, 47.06, 20.57. MS-ESI: calcd for [M + Na]$^+$: 583 (M = $C_{15}H_{19}Cl_2FN_2O_3Pt$), found: 583.

*3.1.2.2 Preparation of compound **2**.* Complex **2** has been prepared in the literature.[31] Herein, it was conveniently synthesized by a different method. Briefly, to a solution of FLP **10** (122 mg, 0.50 mmol) and TBTU (160 mg, 0.50 mmol) in dry DMF 5 mL was added TEA (69 μL, 0.50 mmol) and stirred for 10 min at room temperature. Then, oxoplatin **O1** (66 mg, 0.20 mmol) was added to the solution, and the mixture was further stirred for 48 h at 50 °C in the dark. After that, the solvent was removed under vacuum. The residue was subsequently purified by silica gel column chromatography. Subsequently, pure complex **2** was obtained as a pale solid (66.0 mg, 42%). The NMR and MS data are mainly in accordance with that reported in literature.[31]

^{1}H NMR (500 MHz, DMSO-d_6) δ 7.56–7.50 (m, 4H), 7.50–7.45 (m, 4H), 7.44–7.36 (m, 4H), 7.31–7.20 (m, 4H), 6.69–6.40 (m, 6H), 3.80–3.73 (m, 2H), 1.36 (d, J = 7.1 Hz, 6H). ^{13}C NMR (126 MHz, DMSO-d_6) δ 181.73, 158.27, 144.66, 135.51, 130.65, 129.10, 128.17, 126.67, 124.73, 115.80, 115.62, 46.34, 20.25. MS-ESI: calcd for [M + Na]$^+$: 809 (M = $C_{30}H_{30}Cl_2F_2N_2O_4Pt$), found: 809.

*3.1.2.3 Preparation of compound **3**.* To a solution of FLP **10** (54 mg, 0.22 mmol) and TBTU (71 mg, 0.22 mmol) in dry DMF 5 mL was added TEA (30 μL, 0.22 mmol) and stirred for 10 min at room temperature. Then, oxoplatin **O2** (86 mg, 0.20 mmol) was added to the solution, and the mixture was further stirred for 48 h at 50 °C in the dark. After that, the solvent was removed under vacuum. The residue was subsequently purified by silica gel column chromatography. Subsequently, pure complex **3** was obtained as a pale solid (32.1 mg, 24%).

^{1}H NMR (500 MHz, DMSO-d_6) δ 7.58–7.43 (m, 4H), 7.40 (d, J = 7.2 Hz, 2H), 7.18 (d, J = 11.5 Hz, 2H), 3.76–3.55 (m, 1H), 3.39 (s, 1H), 2.67 (s, 1H), 2.14–1.94 (m, 2H), 1.47 (s, 2H), 1.38–1.21 (m, 4H), 1.09 (t, J = 7.0 Hz, 3H). ^{13}C NMR (126 MHz, DMSO-d_6) δ 182.48, 164.20, 158.30, 144.80, 135.60, 130.82, 129.15, 129.07, 128.16, 124.50, 115.55, 115.37, 65.39, 62.03, 60.36, 47.28, 31.30, 24.12, 19.47, 15.65. MS-ESI: calcd for [M + Na]$^+$: 680 (M = $C_{23}H_{27}FN_2O_7Pt$), found: 680.

*3.1.2.4 Preparation of compound **4**.* To a solution of FLP **10** (122 mg, 0.50 mmol) and TBTU (160 mg, 0.50 mmol) in dry DMF 5 mL was added TEA (69 μL, 0.50 mmol) and stirred for 10 min at room temperature. Then, oxoplatin **O2** (86 mg, 0.20 mmol) was added to the solution, and the mixture was further stirred for 48 h at 50 °C in the dark. After that, the solvent was removed under vacuum. The residue was subsequently purified by silica gel column chromatography. Subsequently, pure complex **4** was obtained as a pale solid (49.4 mg, 28%).

^{1}H NMR (500 MHz, DMSO-d_6) δ 8.69–7.66 (m, 4H, NH_2), 7.57–7.42 (m, 8H), 7.40–7.31 (m, 4H), 7.29–7.07 (m, 4H), 3.91–3.67 (m, 2H), 2.59–2.55 (m, 1H), 2.50–2.37 (m, 1H), 2.29–2.05 (m, 2H), 1.71–1.23 (m, 10H), 1.13–0.87 (m, 2H). ^{13}C NMR (126 MHz, DMSO-d_6) δ 181.86, 178.71, 164.18, 163.11, 160.20, 158.25, 144.93, 144.40, 135.45, 130.82, 129.11, 129.08, 129.06, 129.03, 129.01, 128.99, 128.07, 126.61, 124.50, 119.48, 115.56, 110.22, 61.41, 60.39, 46.08, 23.93, 20.19, 9.04. MS-ESI: calcd for [M + Na]$^+$: 906 (M = $C_{38}H_{38}F_2N_2O_8Pt$), found: 906.

*3.1.2.5 Preparation of compound **5**.* To a solution of ZTP **11** (66 mg, 0.22 mmol) and TBTU (71 mg, 0.22 mmol) in dry DMF 5 mL was added TEA (30 μL, 0.22 mmol) and stirred for 10 min at room temperature. Then, oxoplatin **O2** (66 mg, 0.20 mmol) was added to the solution, and the mixture was further stirred for 48 h at 50 °C in the dark. After that, the solvent was removed under vacuum. The residue was subsequently purified by silica gel column chromatography. Subsequently, pure complex **5** was obtained as a pale solid (26.6 mg, 22%).

^{1}H NMR (500 MHz, DMSO-d_6) δ 8.06 (dt, J = 8.1, 1.9 Hz, 1H), 7.72–7.63 (m, 2H), 7.61–7.53 (m, 1H), 7.52–7.36 (m, 2H), 7.21 (dd, J = 8.0, 1.9 Hz, 1H), 4.31 (d, J = 2.9 Hz, 2H), 3.74 (q, J = 7.1 Hz, 1H), 1.36 (d, J = 7.1 Hz, 3H). ^{13}C NMR (126 MHz, DMSO-d_6) δ 191.11, 175.34, 144.23, 139.82, 137.93, 136.08, 133.50, 132.39, 131.65, 131.42, 131.21, 129.09, 127.64, 127.09, 50.68, 44.72, 18.80. MS-ESI: calcd for [M + Na]$^+$: 637 (M = $C_{17}H_{20}Cl_2N_2O_4PtS$), found: 637.

*3.1.2.6 Preparation of compound **6**.* To a solution of ZTP **11** (149 mg, 0.50 mmol) and TBTU (160 mg, 0.50 mmol) in dry DMF 5 mL was added TEA (69 μL, 0.50 mmol) and stirred for 10 min at room temperature. Then, oxoplatin **O1** (66 mg, 0.20 mmol) was added to the solution, and the mixture was further stirred for 48 h at 50 °C in the dark. After that, the solvent was removed under vacuum. The residue was subsequently purified by silica gel column chromatography. Subsequently, pure complex **6** was obtained as a pale solid (47.6 mg, 27%).

^{1}H NMR (500 MHz, DMSO-d_6) δ 8.12–8.00 (m, 2H), 7.69 (d, J = 7.6 Hz, 2H), 7.67–7.56 (m, 4H), 7.51 (s, 2H), 7.46–7.39 (m, 2H), 7.32–7.21 (m, 2H), 6.48 (br, 6H, NH_3), 4.34–4.24 (m, 2H), 3.43–3.34 (m, 2H), 3.20 (s, 2H), 1.39–1.28 (m, 3H), 1.19–1.09 (m, 3H). ^{13}C NMR (126 MHz, DMSO-d_6) δ 191.48, 181.82, 145.11, 139.90, 137.42, 135.99, 133.54, 131.83, 131.38, 131.21, 131.20, 129.29, 127.64, 127.28, 65.39, 50.63, 49.06, 46.49, 20.11, 15.53. MS-ESI: calcd for [M + Na]$^+$: 917 (M = $C_{34}H_{32}Cl_2N_2O_6PtS_2$), found: 917.

*3.1.2.7 Preparation of compound **7**.* To a solution of ZTP **11** (66 mg, 0.22 mmol) and TBTU (71 mg, 0.22 mmol) in dry DMF

5 mL was added TEA (30 μL, 0.22 mmol) and stirred for 10 min at room temperature. Then, oxoplatin **O2** (86 mg, 0.20 mmol) was added to the solution, and the mixture was further stirred for 48 h at 50 °C in the dark. After that, the solvent was removed under vacuum. The residue was subsequently purified by silica gel column chromatography. Subsequently, pure complex **7** was obtained as a pale solid (45.1 mg, 32%).

^{1}H NMR (500 MHz, DMSO-d_6) δ 8.05 (dt, J = 7.9, 1.4 Hz, 1H), 7.68 (dd, J = 7.9, 1.3 Hz, 1H), 7.62–7.52 (m, 2H), 7.48–7.35 (m, 2H), 7.18 (ddd, J = 10.1, 7.9, 2.0 Hz, 1H), 4.48–4.16 (m, 2H), 3.69 (dq, J = 10.0, 6.9 Hz, 1H), 2.06–1.87 (m, 2H), 1.57–1.32 (m, 4H), 1.32–1.23 (m, 3H), 1.22–0.71 (m, 4H). ^{13}C NMR (126 MHz, DMSO-d_6) δ 191.25, 182.52, 164.25, 164.18, 145.41, 139.92, 137.77, 136.18, 133.46, 131.98, 131.40, 131.32, 131.22, 129.01, 127.62, 127.14, 62.27, 62.00, 60.88, 60.28, 50.66, 47.54, 31.29, 24.07, 19.53. MS-ESI: calcd for $[M + Na]^+$: 734 ($M = C_{25}H_{28}N_2O_8PtS$), found: 734.

3.1.2.8 Preparation of compound ***8****.* To a solution of ZTP **11** (149 mg, 0.50 mmol) and TBTU (160 mg, 0.50 mmol) in dry DMF 5 mL was added TEA (69 μL, 0.50 mmol) and stirred for 10 min at room temperature. Then, oxoplatin **O2** (86 mg, 0.20 mmol) was added to the solution, and the mixture was further stirred for 48 h at 50 °C in the dark. After that, the solvent was removed under vacuum. The residue was subsequently purified by silica gel column chromatography. Subsequently, pure complex **8** was obtained as a pale solid (61.4 mg, 31%).

^{1}H NMR (500 MHz, DMSO-d_6) δ 8.48–8.08 (m, 2H, NH_2), 8.05 (d, J = 7.6 Hz, 1H), 7.99 (d, J = 8.4 Hz, 1H), 7.97–7.77 (m, 2H, NH_2), 7.73 (d, J = 8.4 Hz, 1H), 7.68 (d, J = 7.9 Hz, 1H), 7.63–7.50 (m, 5H), 7.45–7.39 (m, 4H), 7.17 (d, J = 7.4 Hz, 1H), 4.38–3.99 (m, 4H), 3.78 (q, J = 7.1 Hz, 1H), 3.17 (s, 1H), 3.10 (q, J = 7.2 Hz, 1H), 2.16–1.94 (m, 2H), 1.92–1.86 (m, 1H), 1.33–1.29 (m, 3H), 1.27–1.22 (m, 2H), 1.20–1.16 (m, 3H), 1.15–1.04 (m, 2H), 0.89–0.67 (m, 2H). ^{13}C NMR (126 MHz, DMSO-d_6) δ 191.17, 181.38, 163.71, 163.59, 144.70, 139.82, 137.80, 136.14, 133.47, 131.40, 129.05, 128.28, 127.80, 124.98, 119.62, 110.08, 61.28, 50.68, 46.58, 46.24, 31.26, 29.49, 23.79, 19.36, 9.11. MS-ESI: calcd for $[M + H]^+$: 993 ($M = C_{42}H_{40}N_2O_{10}PtS_2$), found: 993.

3.1.2.9 Preparation of compound ***9****.* To a solution of ZTP **11** (66 mg, 0.22 mmol) and TBTU (71 mg, 0.22 mmol) in dry DMF 5 mL was added TEA (30 μL, 0.22 mmol) and stirred for 10 min at room temperature. Then, oxoplatin **O3** (90 mg, 0.20 mmol) was added to the solution, and the mixture was further stirred for 48 h at 50 °C in the dark. After that, the solvent was removed under vacuum. The residue was subsequently purified by silica gel column chromatography. Subsequently, pure complex **7** was obtained as a pale solid (39.1 mg, 27%).

^{1}H NMR (500 MHz, DMSO-d_6) δ 8.08–8.05 (m, 1H), 7.84–7.68 (m, 2H), 7.66–7.53 (m, 2H), 7.53–7.44 (m, 1H), 7.38–7.14 (m, 1H), 4.56–4.19 (m, 2H), 3.90–3.70 (m, 1H), 3.19–3.03 (m, 1H), 2.79–2.62 (m, 1H), 2.16–1.97 (m, 2H), 1.64–1.44 (m, 3H), 1.42–1.34 (m, 1H), 1.30–1.23 (m, 2H), 1.21–1.15 (m, 1H), 1.12–1.03 (m, 2H). ^{13}C NMR (126 MHz, DMSO-d_6) δ 196.00, 187.19, 169.00, 168.93, 150.08, 144.67, 142.47, 140.93, 138.21, 136.61, 136.15, 136.07, 135.97, 133.73, 132.37, 131.89, 66.75, 65.63, 65.03, 55.41, 52.22, 36.04, 28.82, 24.28, 5.33. MS-ESI: calcd for $[M + K]^+$: 769 ($M = C_{25}H_{27}ClN_2O_7PtS$), found: 769.

3.2 Biological evaluation

3.2.1 ***In vitro*** **cellular cytotoxicity assay.** Cells were incubated in culture medium RPMI1640 containing 10% FBS at 37 °C under a humidified atmosphere containing 5% CO_2. The cytotoxic profiles of complexes **1–9**, and reference drugs FLP (**10**), ZTP (**11**), cisplatin and oxaliplatin were tested against six tumor cell lines including human ovarian cancer (SKOV-3), human lung cancer (A549), cisplatin-resistant human lung cancer (A549R), human liver cancer (HepG2), murine breast cancer (4T1), murine colon cancer (CT-26), and one human normal liver cell line (LO2) using a MTT assay.

Briefly, 5×10^3 cells in 100 μL of medium were seeded per well in 96-well plates, and preincubated for 12 h. Then, the cells were exposed to the tested complexes for 48 h. After that, 20 μL of freshly prepared MTT solution (5 mg mL^{-1} in PBS) were added and further incubated for 4 h. The culture medium was removed and DMSO (150 μL) was added to dissolve the purple formazan crystals. Absorbance of the solution was quantified using a microplate reader at 570 nm (TECAN Spark). The IC_{50} values were calculated based on three parallel experiments using GraphPad Prism 6.

3.2.2 ***In vivo*** **antitumor assay.** The mice were purchased from Pengyue Experimental Animal Company (Jinan, China). All mice had access to food and water *ad libitum* with a 12–12 h light cycle, and were maintained under controlled temperature (23 ± 2 °C). All the animal experiments were performed in strict accordance with the NIH guidelines for the care and use of laboratory animals (NIH Publications No. 8023, revised 1978) and were approved by the Institute Animal Ethics Committee of Liaocheng University.

The antitumor activities against CT-26 tumors *in vivo* were evaluated on male BALB/c mice (18–20 g). CT-26 cells (1×10^6 in 0.15 mL PBS) were injected subcutaneously into the left flank of mice. The mice were randomly divided into seven groups (n = 6) on day 3 when the tumor nodules were palpable. The mice were treated with **1**, **2**, **5**, **6**, cisplatin, oxaliplatin (4 mg Pt per kg, i.p.) and saline (blank), respectively. The drugs were administered four times on days 3, 6, 9, and 12 posttumor inoculation, and the tumor volume (V) was monitored as $V = L \times W^2/2$, where the length (L) and width (W) were measured. The mice were sacrificed on day 17. The blood and tissues including liver, heart, spleen, lung and kidney were collected. The tumors were weighed and the growth inhibition rate (TGI) was calculated as follows: TGI (%) = [(average tumor weight of blank group − average tumor weight of the drug treated group)/(average tumor weight of blank group)] × 100%. The tumors and organs were formalin-fixed, paraffin-embedded, and cut with a microtome (5 μm sections) for

hematoxylin and eosin (H&E) staining and immunohistochemical detection.

Then the antitumor activities of complexes **1** and **2** against 4T1 homograft tumors were further tested on female BALB/c mice (18–20 g). Murine 4T1 cells (1×10^6 in 0.15 mL PBS) were injected subcutaneously into the flank of BALB/c mice, and the mice were divided into five groups on day 3 ($n = 5$). Complex **1** (4 mg Pt per kg), **2** (4 mg Pt per kg), cisplatin (2 mg Pt per kg), oxaliplatin (4 mg Pt per kg) and blank (saline) were administered four times on days 3, 6, 9 and 12. Mice were euthanized on day 15. The data were collected and analysed as mentioned above.

To compare the antitumor properties of flurbiprofen and zaltoprofen platinum(IV) complexes with those of ketoprofen and loxoprofen platinum(IV) complexes reported in our previous work,[29] the anti-proliferation and anti-metastasis experiments were carried out at the same time with the same negative control group (blank group).

3.2.3 *In vivo* anti-metastasis assay. The anti-metastasis experiment *in vivo* was performed on female BALB/c mice (18–20 g). Pulmonary metastasis models were established by the injection of 4T1 cells (2×10^5 in 0.1 mL PBS) *via* the tail vein. Then, drugs **1**, **2**, cisplatin and oxaliplatin were given on days 2, 4, 6, 8, 10, 12 and 14 for 7 times at dosage of 2 mg Pt per kg (i. p.). The saline group was set as blank. The mice were euthanized on day 14 after the last administration. The lungs were collected and fixed with Bouin's fluid for 24 h. The pulmonary metastasis nodules on each lung were counted and analysed. Then the lung slices were stained by H&E.

3.2.4 AST, ALT, BUN and CRE detection. The serum samples were collected after centrifuging at 1500*g* for 15 min, and stored at −80 °C. Then, the AST, ALT, BUN and CRE were detected using Elisa kits (Nanjing Jiancheng Bioengineering Institute, China) according to the given protocols. The OD values were recorded on an automatic microplate reader (Tecan Spark).

3.2.5 Wound healing assay. The 4T1 cells (8×10^5) were incubated in 6-well cell culture plate for 12 h at 37 °C. After the cells grew to 90% confluency, a wound was created in each well. Then, complex **2** (2 μM), cisplatin (10 μM) and oxaliplatin (10 μM) were added. The untreated well was set as blank. The images of the wound were photographed at 0 h, 12 h and 24 h.

3.2.6 Transwell migration assay. The transwell migration experiment was carried out using a 24-well chamber (Costar 3422) containing inserts (8 μm pores). Briefly, 4T1 cells (5×10^4) in 0.2 mL RPMI1640 medium were seeded in the upper compartment of the chamber, and 0.6 mL culture media of RPMI1640 with 10% FBS were added in the lower compartment. Complex **2** (2 μM), cisplatin (2 μM) and oxaliplatin (10 μM) were added into the culture media in the lower compartment, and the cells were further incubated for 24 h. Then cells were fixed in 4% paraformaldehyde for 20 min, and stained with 0.1% crystal violet for 20 min. The non-migrating cells in the upper chamber were scraped away using a cotton swab, and the migrated cells on the lower surface were photographed with an inverted microscope (Olympus) in five random visual fields and the migrated cells were measured using Image J.

3.2.7 Apoptosis experiment–Annexin V-FITC/PI assay. The apoptosis-inducing properties were evaluated using an Annexin V-FITC/PI apoptosis detection kit (Beyotime Biotechnology, China). The experiments were carried out according to the given protocol. Briefly, A549 cells 2×10^5 were seeded in a 6-well cell culture plate and incubated for 12 h. Then, drugs **1** (10 μM), **2** (5 μM), **5** (10 μM), **6** (10 μM), cisplatin (10 μM), oxaliplatin (10 μM) were added and the cells were further incubated for 24 h. After that, the cells were harvested, stained by annexin V-FITC and propidium iodide (PI), and analysed by flow cytometric assay.

3.2.8 HPLC assay. The HPLC test was performed on a Thermo Ultimate 3000 RS equipped with an Agilent Eclipse XDB-C18 column (250 × 4.6 mm, 5 μm). The flow rate was 1.0 mL min^{-1}, and the injection volume was 10 μL. The HPLC spectra were recorded by a diode array detector. The linear gradient is given in Table 2.

The stability of complex **2** (0.5 mM) in PBS and RPMI1640 was examined for 24 h at 37 °C. To determine whether the FLP platinum(IV) complex could be reduced in TME, the solution of complex **2** (0.25 mM) in PBS with ascorbic acid (AsA, 1 mM, similar concentration as in TME) was recorded. Then, guanosine 5′-monophosphate disodium (5′-GMP) was added as a model of DNA base, and the solution containing complex **2** (0.5 mM), 5′-GMP (3 mM), and AsA (1 mM) was measured by HPLC to determine the DNA-binding properties.

The whole-blood stability test was carried out in fresh blood of BALB/C mice with heparin. Complex **2** (1 mM) in blood was incubated at 37 °C. A 100 μL aliquot of the blood sample was taken at different time points (0 h, 1 h, 2 h, 4 h, 5 h, and 12 h). The blood was extracted with 300 μL of octanol, and examined by HPLC. The half-life time ($t_{1/2}$) in blood was calculated.[41]

3.2.9 Mitochondrial membrane potential experiment–JC-1 assay. The mitochondrial membrane potential of A549 cells treated by different drugs was tested by JC-1 assay using a Mitochondrial Membrane Potential Assay Kit (JC-1) (Solarbio, China). Cells (2×10^5) were seeded in a 6-well cell culture plate and pre-incubated for 12 h. Complexes **1** (10 μM), **2** (5 μM), **5** (10 μM), **6** (10 μM), cisplatin (10 μM) and oxaliplatin (10 μM) were added and the cells were further incubated for another 24 h. After that, all cells were harvested, stained by JC-1, and tested by flow cytometry.

3.2.10 ROS experiment–DCFH-DA assay. The ROS production in tumor cells was tested by DCFH-DA assay. Briefly,

Table 2 The linear gradient for HPLC

Time (min)	*A* (0.1% aqueous TFA)	*B* (methol)
0	90	10
5	90	10
25	30	60
26	10	90
34	10	90

A549 cells (2×10^5) were seeded in a 6-well cell culture plate and pre-incubated for 12 h. Then, complexes **1** (10 μM), **2** (5 μM), **5** (10 μM), **6** (10 μM), cisplatin (10 μM) and oxaliplatin (10 μM) were added and further incubated for 24 h. After that, cells were stained with DCFH-DA (10 μM) for 20 min, and imaged with a fluorescence microscope (Olympus IX73) under visible light and blue light, respectively. For the flow cytometric assay, all the cells were harvested after treated with different drugs for 24 h. Then, cells were stained with DCFH-DA (10 μM) for 20 min, washed twice with cold PBS, and detected immediately by flow cytometry.

3.2.11 Western blot assay. The A549 cells were cultured and treated with complex **1** (10 μM), **2** (5 μM) and cisplatin (10 μM) for 24 h at 37 °C and harvested. The cells were lysed and measured using a BCA assay (Sangon Biotec, China). Proteins with loading buffer were loaded and separated on 10% sodium dodecyl sulfate-polyacrylamide gel electrophoresis (SDS-PAGE) (Sangon Biotec, China), and then transferred onto PVDF membrane (Millipore). The membrane was blocked with 5% nonfat milk for 1 h, incubated with primary antibodies overnight at 4 °C and secondary antibodies for 2 h at room temperature. Finally, the membrane was treated with an ECL western blotting substrate kit (ProteinTech, China), and imaged by a scanning system (Tanon 46000SF). Primary antibodies γ-H2AX (Ser139) (Cell signaling Technology, USA), p53 (SANTA CRUZ Biotechnology, USA), Bcl-2 (ProteinTech, China), Bax (Servicebio, China), caspase3 (ProteinTech, China), *c*-caspase3 (Abcam, England), COX-2 (Abcam, England), MMP-9 (ProteinTech, China), NLRP3 (ABclonal Technolog, China) and caspase1 (ABclonal Technolog, China) were used.

3.2.12 Immunohistochemical assay. Proteins COX-2, MMP-9, PD-L1, $CD3^+$ and $CD8^+$ expressed in tumor tissues were detected by immunohistochemical assay. The slices of tumor tissues were deparaffinized, hydrated, boiled in citrate buffer under microwave, and further blocked for 60 min in 10% normal goat serum. The slices were treated with primary antibody COX-2 (Servicebio, China), MMP-9 (Servicebio, China), PD-L1 (Servicebio, China), $CD3^+$ (Servicebio, China) and $CD8^+$ (Servicebio, China) overnight at 4 °C. Then, the sections were incubated with secondary antibody (Servicebio, China) for 50 min at room temperature. After that, the sections were visualized with 3,3′-diaminobenzidine (DAB) (Servicebio, China) and counterstained with hematoxylin.

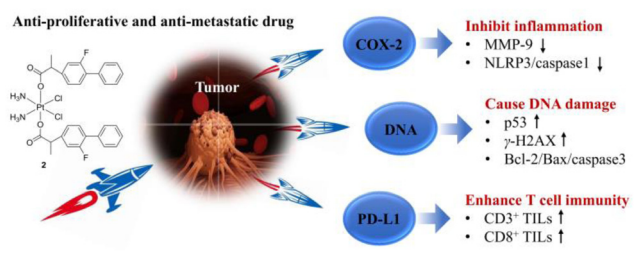

Fig. 15 The proposed antitumor mechanism for FLP platinum(IV) complexes targeting COX-2, PD-L1 and DNA.

4. Conclusion

In this work, a series of FLP and ZTP platinum(IV) complexes targeting COX-2, PD-L1 and DNA was prepared and evaluated as antitumor agents with both anti-proliferative and anti-metastatic competence. Title platinum(IV) complexes especially **1**, **2**, **5** and **6** with cisplatin core, display potent antitumor activities *in vitro*, and show great potential in defeating cisplatin resistance. Further antitumor activities *in vivo* demonstrate that FLP platinum(IV) complex **2** exerts the most potent tumor growth suppression against the homograft tumors CT26 and 4T1 which is comparable or even superior to the platinum(II) reference drugs, but induces rather lower toxicities. More encouragingly, it displays satisfactory metastasis-inhibitory properties *in vivo* with a significantly higher inhibition rate of metastatic nodules (86.3%) than cisplatin (65.5%) and oxaliplatin (40.7%). Detection of the mechanism (Fig. 15) reveals that complex **2** could be easily reduced to platinum(II) complexes in reducing TME and further cause serious DNA damage. Proteins γ-H2AX and p53 as DNA damage indicators are up-regulated in tumor cells. Apoptosis of tumor cells is promoted by complex **2** through activating the Bcl-2/Bax/caspase3 mitochondrial pathway and enhancing ROS generation. Furthermore, the tumor-recruited inflammation could be restrained by suppression of key enzymes COX-2, MMP-9, NLRP3 and caspase1. These action procedures synergistically facilitate complex **2** to overcome drug resistance of cisplatin. Moreover, compound **2** is of great potential in elevating the T-cell immunity in TME by inhibiting PD-L1 expression, and further improving the density of $CD3^+$ and $CD8^+$ T cells in tumor tissues. Accordingly, all these effects enable FLP platinum(IV) complex **2** be worthy of further development as a new anticancer and anti-metastatic drug, and further expands the applications of NSAIDs platinum(IV) complexes in curing metastatic cancers.

Author contributions

ZLi: investigation, formal analysis and writing – original draft; LL, WZ, BS, ZLiu, ML, JH, ZW and DL: investigation and writing – review & editing; QW: conceptualization, funding acquisition, supervision, investigation and writing – review & editing.

Conflicts of interest

There are no conflicts to declare.

Acknowledgements

This work was supported by the Natural Science Foundation of Shandong Province (No. ZR2020KH005), the Youth Innovative Science and Technology Program of Shandong Colleges and University (No. 2021KJ099) and the National Natural Science

Foundation of China (No. 21807056). This work was also technically supported by the Shandong Collaborative Innovation Center for Antibody Drugs, the Engineering Research Centre for Nanomedicine and Drug Delivery Systems and Taishan Scholar Research Group.

References

1 X. M. Guan, *Acta Pharm. Sin. B*, 2015, **5**, 402–418.
2 C. Sonnenschein and A. M. Soto, *J. Natl. Cancer Inst.*, 2015, **107**, djv236.
3 C. A. Klein, *Nat. Rev. Cancer*, 2020, **20**, 681–694.
4 G. Bergers and S. Fendt, *Nat. Rev. Cancer*, 2021, **21**, 162–180.
5 B. K. Gersten, T. S. Fitzgerald, K. A. Fernandez and L. L. Cunningham, *J. Assoc. Res. Otolaryngol.*, 2020, **21**, 303–321.
6 E. Wong and C. M. Giandomenico, *Chem. Rev.*, 1999, **99**, 2451–2466.
7 T. C. Johnstone, K. Suntharalingam and S. J. Lippard, *Chem. Rev.*, 2016, **116**, 3436–3486.
8 X. Tan, G. Li, Q. Wang, B. Wang, D. Li and P. G. Wang, *Prog. Chem.*, 2018, **30**, 831–846.
9 C. Jia, G. B. Deacon, Y. Zhang and C. Gao, *Coord. Chem. Rev.*, 2020, **429**, 213640.
10 R. G. Kenny and C. J. Marmion, *Chem. Rev.*, 2019, **119**, 1058–1137.
11 Q. Wang, Y. Chen, G. Li, Z. Liu, J. Ma, M. Liu, D. Li, J. Han and B. Wang, *Bioorg. Med. Chem.*, 2019, **27**, 2112–2121.
12 G. Li, J. Zhang, Z. Liu, Q. Wang, Y. Chen, M. Liu, D. Li, J. Han and B. Wang, *J. Inorg. Biochem.*, 2019, **194**, 34–43.
13 X. Wang, X. Wang and Z. Guo, *Acc. Chem. Res.*, 2015, **48**, 2622–2631.
14 D. Hanahan and R. A. Weinberg, *Cell*, 2011, **144**, 646–674.
15 T. Wu and Y. Dai, *Cancer Lett.*, 2017, **387**, 61–68.
16 O. Trédan, C. M. Galmarini, K. Patel and I. F. Tannock, *J. Natl. Cancer Inst.*, 2007, **99**, 1441–1454.
17 S. I. Grivennikov, F. R. Greten and M. Karin, *Cell*, 2010, **140**, 883–899.
18 J. Terzić, S. Grivennikov, E. Karin and M. Karin, *Gastroenterology*, 2010, **138**, 2101–2114.
19 Y. Chen, Q. Wang, Z. Li, Z. Liu, Y. Zhao, J. Zhang, M. Liu, Z. Wang, D. Li and J. Han, *Dalton Trans.*, 2020, **49**, 5192–5204.
20 S. Jin, N. Muhammad, Y. Sun, Y. Tan, H. Yuan, D. Song, Z. Guo and X. Wang, *Angew. Chem., Int. Ed.*, 2020, **59**, 23313–23321.
21 R. Pathak, S. Marrache, J. H. Choi, T. B. Berding and S. Dhar, *Angew. Chem.*, 2014, **126**, 1994–1998.
22 Q. Cheng, H. Shi, H. Wang, Y. Min, J. Wang and Y. Liu, *Chem. Commun.*, 2014, **50**, 7427–7430.
23 Q. Cheng, H. Shi, H. Wang, J. Wang and Y. Liu, *Metallomics*, 2016, **8**, 672–678.
24 W. Neumann, B. C. Crews, M. B. Sarosi, C. M. Daniel, K. Ghebreselasie, M. S. Scholz, L. J. Marnett and E. Hey-Hawkins, *ChemMedChem*, 2015, **10**, 183–192.
25 L. Li, Y. Chen, Q. Wang, Z. Li, Z. Liu, X. Hua, J. Han, C. Chang, Z. Wang and D. Li, *Int. J. Nanomed.*, 2021, **16**, 5513–5529.
26 P. Sharma and J. P. Allison, *Science*, 2015, **348**, 56–61.
27 A. Akinleye and Z. Rasool, *J. Hematol. Oncol.*, 2019, **12**, 92.
28 F. K. Dermani, P. Samadi, G. Rahmani, A. K. Kohlan and R. Najafi, *J. Cell Physiol.*, 2019, **234**, 1313–1325.
29 Z. Li, Q. Wang, L. Li, Y. Chen, J. Cui, M. Liu, N. Zhang, Z. Liu, J. Han and Z. Wang, *J. Med. Chem.*, 2021, **64**, 17920–17935.
30 C. Bailly and G. Vergoten, *Biochem. Pharmacol.*, 2020, **178**, 1140–1142.
31 J. Tan, C. Li, Q. Wang, S. Li, S. Chen, J. Zhang, P. C. Wang, L. Ren and X. Liang, *Mol. Pharmaceutics*, 2018, **15**, 1724–1728.
32 J. García-González, J. Ruiz-Bañobre, F. J. Afonso-Afonso, M. Amenedo-Gancedo, M. C. Areses-Manrique, B. Campos-Balea, J. Casal-Rubio, N. Fernández-Núñez, J. L. F. Pérez, M. Lázaro-Quintela, D. P. Parente, L. Crama, P. Ruiz-Gracia, L. Santomé-Couto and L. León-Mateos, *J. Clin. Med.*, 2020, **9**, 2093.
33 Q. Wang, X. Tan, Z. Liu, G. Li, R. Zhang, J. Wei, S. Wang, D. Li, B. Wang and J. Han, *Eur. J. Pharm. Sci.*, 2018, **124**, 127–136.
34 Z. Liu, Z. Li, T. Du, Y. Chen, Q. Wang, G. Li, M. Liu, N. Zhang, D. Li and J. Han, *Dalton Trans.*, 2021, **50**, 362–375.
35 Q. Wang, Z. Huang, J. Ma, X. Lu, L. Zhang, X. Wang and P. G. Wang, *Dalton Trans.*, 2016, **45**, 10366–10374.
36 Q. Wang, G. Li, Z. Liu, X. Tan, Z. Ding, J. Ma, L. Li, D. Li, J. Han and B. Wang, *Eur. J. Inorg. Chem.*, 2018, **40**, 4442–4451.
37 Q. Wang, Y. Chen, G. Li, Y. Zhao, Z. Liu, R. Zhang, M. Liu, D. Li and J. Han, *Bioorg. Med. Chem. Lett.*, 2019, **29**, 126670.
38 Z. Li, Y. Chen, Z. Liu, Q. Wang, Y. Zhao, J. Wei, M. Liu, Z. Wang, D. Li and J. Han, *Monatsh. Chem.*, 2020, **151**, 353–367.
39 J. Ma, Q. Wang, Z. Huang, X. Yang, Q. Nie, W. Hao, P. G. Wang and X. Wang, *J. Med. Chem.*, 2017, **60**, 5736–5748.
40 R. Oun, Y. E. Moussa and N. J. Wheate, *Dalton Trans.*, 2018, **47**, 6645–6653.
41 D. X. Nguyen, P. D. Bos and J. Massague, *Nat. Rev. Cancer*, 2009, **9**, 274–284.
42 S. G. Awuah, Y. Zheng, P. M. Bruno, M. T. Hemann and S. J. Lippard, *J. Am. Chem. Soc.*, 2015, **137**, 14854–14857.
43 V. Petrilli, *Curr. Opin. Oncol.*, 2017, **29**, 35–40.
44 M. J. Daniels, J. Rivers-Auty, T. Schilling, N. G. Spencer, W. Watremez, V. Fasolino, J. Sophie, S. J. Booth, C. S. White, A. G. Baldwin, S. Freeman, R. Wong, C. Latta, S. Yu, J. Jackson, N. Fischer, V. Koziel, T. Pillot, J. Bagnall, S. M. Allan, P. Paszek, J. Galea, M. K. Harte, C. Eder, C. B. Lawrence and D. Brough, *Nat. Commun.*, 2016, **7**, 12504.

45 G. Kroemer, L. Galluzzi, O. Kepp and L. Zitvogel, *Annu. Rev. Immunol.*, 2013, **31**, 51–72.
46 L. Xia, Y. Liu and Y. Wang, *Oncologist*, 2019, **24**, S31–S41.
47 J. Cha, L. Chan, C. Li, J. L. Hsu and M. Hung, *Mol. Cell*, 2019, **76**, 359–370.
48 V. Prima, L. N. Kaliberova, S. Kaliberov, D. T. Curiel and S. Kusmartsev, *Proc. Natl. Acad. Sci. U. S. A.*, 2017, **114**, 1117–1122.
49 G. Botti, F. Fratangelo, M. Cerrone, G. Liguori, M. Cantile, A. M. Anniciello, S. Scala, C. D'Alterio, C. Trimarco, A. Ianaro, G. Cirino, C. Caracò, M. Colombino, G. Palmieri, S. Pepe, P. A. Ascierto, F. Sabbatino and G. Scognamiglio, *J. Transl. Med.*, 2017, **15**, 46.
50 X. Jiang, J. Wang, X. Deng, F. Xiong, J. Ge, B. Xiang, X. Wu, J. Ma, M. Zhou, X. Li, Y. Li, G. Li, W. Xiong, C. Guo and Z. Zeng, *Mol. Cancer*, 2019, **18**, 10.